



LAWRENCE  
LIVERMORE  
NATIONAL  
LABORATORY

# Investigation of Laser Coupling for Impulse Generation

K. Fournier

September 6, 2012

## **Disclaimer**

---

This document was prepared as an account of work sponsored by an agency of the United States government. Neither the United States government nor Lawrence Livermore National Security, LLC, nor any of their employees makes any warranty, expressed or implied, or assumes any legal liability or responsibility for the accuracy, completeness, or usefulness of any information, apparatus, product, or process disclosed, or represents that its use would not infringe privately owned rights. Reference herein to any specific commercial product, process, or service by trade name, trademark, manufacturer, or otherwise does not necessarily constitute or imply its endorsement, recommendation, or favoring by the United States government or Lawrence Livermore National Security, LLC. The views and opinions of authors expressed herein do not necessarily state or reflect those of the United States government or Lawrence Livermore National Security, LLC, and shall not be used for advertising or product endorsement purposes.

This work performed under the auspices of the U.S. Department of Energy by Lawrence Livermore National Laboratory under Contract DE-AC52-07NA27344.

# INVESTIGATION OF LASER COUPLING FOR IMPULSE GENERATION

## SUBCONTRACT NO. B596804

between

LAWRENCE LIVERMORE NATIONAL SECURITY, LLC

and

ALME AND ASSOCIATES

### **1 Objective**

The goal of the proposed work is to develop new laser-target configurations such that with the appropriate laser irradiation parameters (intensity, pulse-shape, pulsewidth) and target design, the induced stress (shock) wave in test materials simulates that which would result from absorption of an intense x-ray pulse. We will develop new target configurations using added 'laser coupling/tamping' layer(s) to materials under test to increase and to tailor the laser-induced impulse. The successful completion of the proposed research will develop new capabilities and techniques that will provide cost effective techniques to allow assessment of new aeroshell materials and aeroshell configurations for strategic applications and allow measurement of key material properties, thus providing basic data needed for detailed modeling and simulation that can be extrapolated to threat conditions.

### **2 Task Statements**

Task 1: Plan and design experimental campaign on the LLNL Janus laser of the Jupiter Laser Facility in coordination with LLNL,

Task 2: Conduct two experimental campaigns (order of 1-week tests each),

Task 3: Analyze and document results.

### **3 Description of Experiment**

Team:

Kevin Fournier - LLNL

John F Davis – Alme and Associates

Steven W. Seiler - Alme and Associates

Mr. Jim Emig – LLNL

Andrew Sibley – AWE

Adrian Hughes– AWE

The basic objective of the proposed research is development of new techniques to tailor the laser-induced blow-off impulse to allow parametric studies of material response to measure basic material properties to support high fidelity M&S. The initial objective is to measure the laser-induced impulse as a function of the laser intensity and pulsewidth with known materials and to

establish techniques to study the effects of ‘laser coupling/tamping’ layer(s) added to the targets in order to increase and tailor the laser-induced impulse. Then, using these new techniques, the follow-on objective is to study the shock properties of new materials and/or material configurations relevant for defense applications.

Previous work by Kevin Fournier (part of this research team) has measured impulse data for laser interaction with pure aluminum and carbon targets. However, in those experiments, there were limitations on the available laser test time and the available laser pulsewidth (limited to ~1.5 ns or less). Those data compare well with the previous documented work. The paper by Claude Phipps, et al (see references) summarizes and analyzes previous work up to 1988 on laser impulse coupling to simple targets in vacuum, but for a limited range of conditions and materials. Their analysis has yielded insights into the coupling efficiency and they derived a mechanical coupling coefficient  $C_m$ :

$$C_m = P_a / I_{laser} = J / E_{laser}$$

$$J = C_m \cdot E_{laser}$$

where  $P_a$  = ablation pressure (dyn-cm<sup>2</sup>)  
 $I_{laser}$  = incident laser intensity W/cm<sup>2</sup>)  
 $J$  = total momentum imparted to the target (dyn-s), and  
 $E_{laser}$  = laser energy (J/cm<sup>2</sup>)

For Aluminum alloys;  $C_m \approx 5.58 (I\lambda\sqrt{\tau})^{-0.3}$ ,  
 where  $\lambda$  is the laser wavelength (cm) and  $\tau$  is the laser pulse width (s).

Previously measured values of  $C_m$  are of order 0.2 – 5, but for the range of available parameter space with the Janus laser,  $C_m$  will be of order 0.6-0.8. Our objective is to continue the work initiated by Dr. Fournier to develop new targets using ‘laser coupling/tamping’ layer(s) to increase the laser coupling efficiency and to also allow control of the induced stress impulse shape that can be compared to x-ray induced stress waves typical of threat conditions. In the paper by Phipps, et. al, they discuss the potential advantages of laser light absorbed in-depth in a semi-opaque material, and postulate that the mechanical coupling should be more efficient than with surface absorption. However, they note that no experiments have been performed to validate this hypothesis. We proposed a phased experimental and modeling approach to validate this hypothesis.

As an example of the potential capability, assuming a neodymium(Nd)-glass laser ( $\lambda=1.6 \times 10^{-4}$  cm at 1 $\omega$ ) with a 1.5ns pulse, at 120 J/cm<sup>2</sup>,  $8 \times 10^{10}$  W/cm<sup>2</sup>, the calculated coupling coefficient is  $\approx 0.97$ . Using the equation above, the calculated impulse is  $\approx 120$  taps. Now, compare to a 1 keV Blackbody radiation spectrum with a 10 ns pulsewidth. At 120 J/cm<sup>2</sup> (28.7 cal/cm<sup>2</sup>) the impulse is  $\approx 1250$  taps or over 10X. The x-ray impulse is greater because of the greater penetration depth that couples with more surface material. Adding a coupling layer to the surface of a laser target material that allows a greater laser penetration depth should likewise be able to increase  $C_m$ .

## 3.1 Facilities & Test Configuration

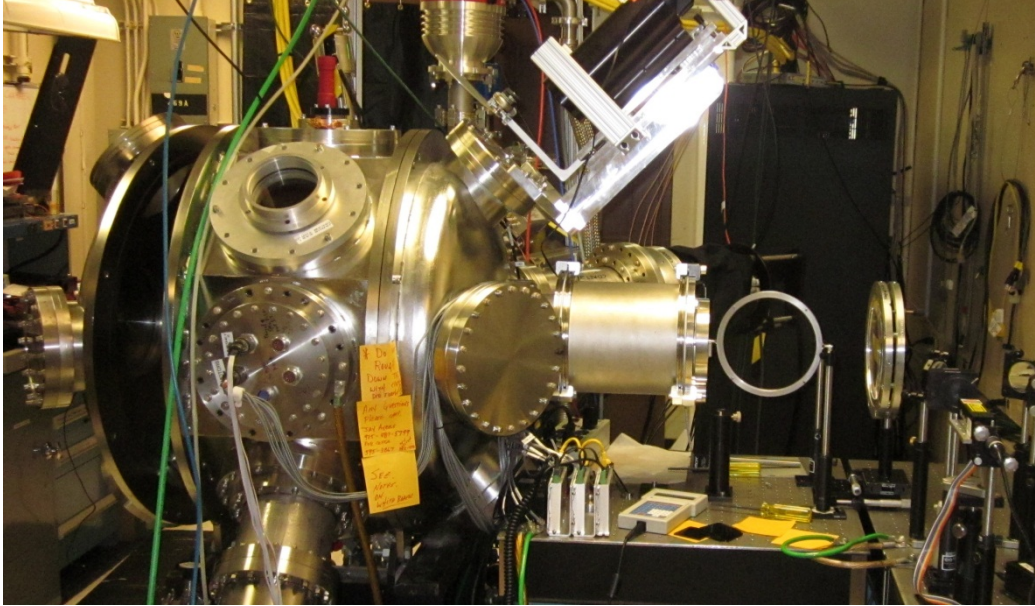
### 3.1.1 Laser

The Janus laser operation is administered by the LLNL Jupiter Laser Facility. The Janus laser is a two beam flashlamp pumped Nd glass laser system that can be operated in  $1\omega$  and  $2\omega$  with peak energies of order 1 kilojoule. For our experiments, we utilized target area 1 (TA1) and for this target area, Janus is at present limited to one beam, at  $1\omega$  with standard pulse shapes, pulse widths of 1.5 ns, 5ns, 10ns and 20ns, laser energies of order 200J.

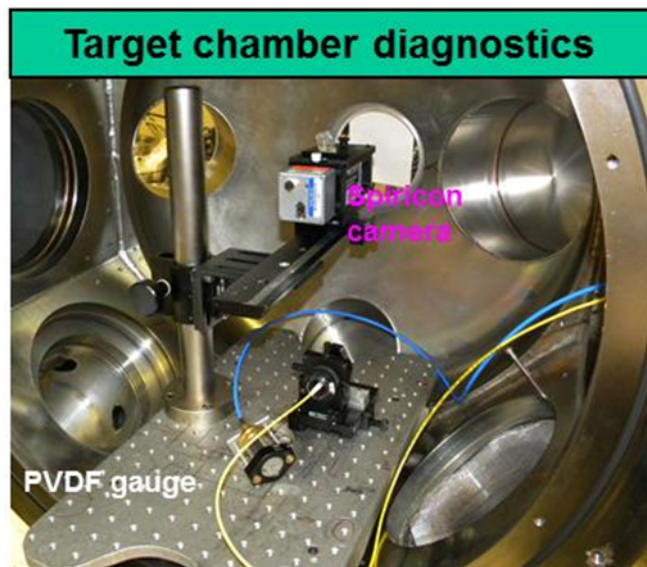
### 3.1.2 Test Stand

Figure 1 shows the target chamber in TA-2. The chamber opens on the left side of the figure to allow easy access to the target area. The laser beam enters the target area through the South wall to a  $90^\circ$  turning mirror to a final focus lens external to the target chamber. At the target chamber there is a laser entrance window and mounted just behind the window is a thin ( $\sim 1\text{mm}$ ) debris shield. All of the light transmission surfaces are AR coated and the turning mirror is optimized for  $1\omega$ . An estimate of the actual laser energy to the target from a measurement at a pickoff in the laser bay assuming 99% transmission and/or reflections per surface implies (two mirrors, one lens, two windows) is  $0.99^8$  is  $\sim 92.3\%$ . When the beam is diverted from TA-1 to TA-2, it bypasses all the energy diagnostics. Thus, for some of the early laser shots, a calorimeter was set up external to the target chamber laser entrance window to allow across calibration to the laser bay pickoff.

Figure 2 shows the target holder assembly and the diagnostic systems used for the experiments. The Spiricon camera was used to measure the laser beam profile versus spot size. For laser impulse shots, a simple optic holder held the targets (1" diameter) with either a PVDF gauge attached to the target or a fiber optic based photo-displacement interferometer system (PDI). The holder for the fiber optic for laser interferometer was a precision x-y and crude z alignment holder.



**Figure 1:** Target chamber in TA1



**Figure 2:** Interior target chamber setup.

### 3.1.3 Targets

The laser targets were of simple designs to ensure one-dimensional shock propagation over the measurement times of interest. The initial targets used Al-6061 with a well-known EOS. The general design of targets will consist of 1) test material, backed by 2) a standard diagnostic configuration, with 3) a laser coupling/tamping material on the front of the test material, and finally, 4) optional coupling enhancement layer(s). A cross-sectional view of the proposed targets is shown in the Figure 3. In order to maintain one-dimensional response of the shock-wave diagnostic (a photon-displacement interferometer (PDI) – see reference by S. Jones, and/or a piezo-electric (PVDF) strain gauge) over the desired period of the shock-response measurement the minimum target diameter must ensure that the shock relief from the sides of the target do not compromise the measurement. Assuming measurement duration of one transit time through the thickness of the target disk, one can specify the minimum disk diameter assuming a

reasonable uncertainty margin,  $R$ , given by;

$$D_{\min} > d + 2(Rh)$$

For detector spot size  $d$  of order 3 mm and target thickness  $h$  of order 1.5 mm (60 mils) and with a margin  $R$  of  $\sim 1.5$ , the minimum diameter for a uniform impulse  $D_{\min} > 7.5$  mm (+ 2w).

Revision for Janus to TA2:  $d \sim 1.3$  mm (to include some margin of error)  
 $h = 1$  mm;  $R \sim 1.3$

$$D_{\min} > 4\text{mm}$$

Thus a requirement for these experiments is to have a relatively flat intensity profile onto the target with a spot of order 4 mm diameter or larger. The basic test package is envisioned to have test material thicknesses of order 1 mm, with coupling/ablation layers and coupling enhancement layers of order 10 – 50 microns each. Each laser experiment will generate debris of order <15 mg of mid- to low- $Z$  material per shot (the ablation layer). The final experimental setup must account for effects of this amount of debris into the target chamber per shot.

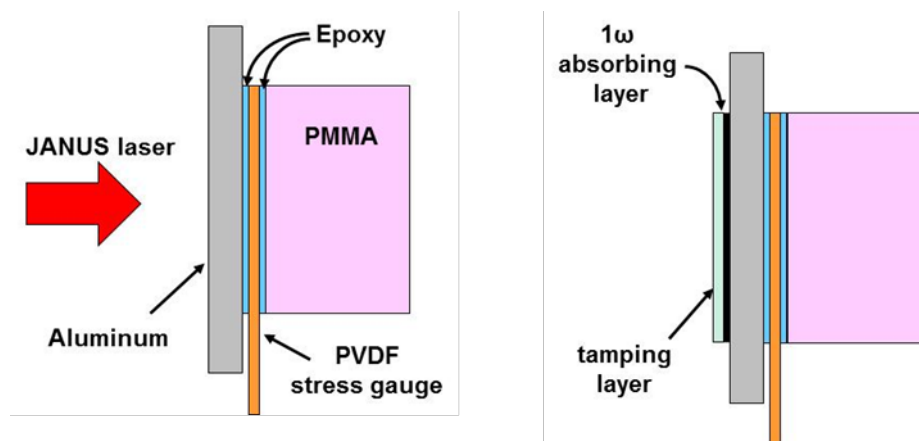


**Figure 3:** Target construction for the PVDF diagnostic.

### 3.1.4 Diagnostics

The test team supplied all the required diagnostics to measure the laser induced shock in the test objects. There were two systems to measure the target response. These were simple commercial piezo-electric stress gauges and a Photonic Displacement Interferometer (PDI), a fiber optic based system, which uses an external laser to the target chamber and coupled to the test object via fiber optic. The AWE team of Andy Sibley and Adrian Hughes setup and operated the PDI diagnostic. Some additional information on the system is in the appendix or refer to the information from Scott Jones of SNL (see references). The PDI system was the primary diagnostic for Janus I.

For the second data series, Janus II, the primary diagnostic was the PVDF stress gauge mounted as shown in Figure 3 with Figure 4 showing an assembled target. The PVDF gauges were from Dynasen, Inc, Goleta, CA, ([www.dynasen.com](http://www.dynasen.com)), part # PVF2-11-.040-EK. The gauge design is shown in Figure 5, with the PVF2 thickness of 0.0011 inches (27.94 microns) and element size 0.040x0.040 (1x1mm). The Kapton (polyimide) was 0.001 inch top and bottom (25.4 microns).

The PVDF gauge was mounted between the aluminum target and the PMMA back with thin layers of epoxy, Loctite Hysol Adhesive Cartridge, E-30CL Glass Bonder Epoxy, 1.69 oz (50 ml) (McMaster-Carr, part #6430A23).



**Figure 4:** Photo of assembled target with PVDF stress gauge. Target is 25mm diameter Al-6061, 954 micron thick, with 3.18mm thick PMMA back plate.

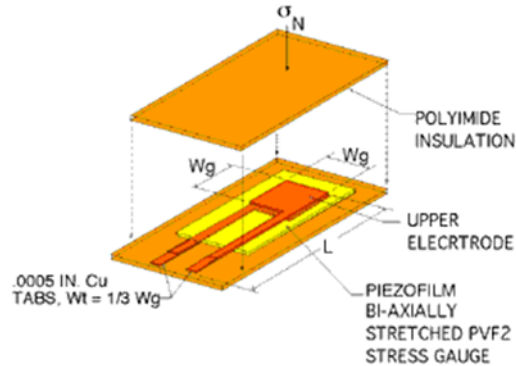


**Figure 5:** Schematic of the design of the PVDF gauge from Dynasen, Inc.

Figure 4 shows a photo of assembled target with PVDF stress gauge. The target diameter is 25mm, Al-6061, 954 micron thick, with 3.18mm thick PMMA back plate. Note that the PVDF is a non-conductor with two electrical leads on either side as shown in the figure and therefore the gauge is subject to electromagnetic noise produced during the experiment. For all our experiments we mounted the gauge in a shielded container with the two leads to a SMA connector (see Figure 2) that was grounded to the target chamber at the vacuum feedthru.

The gauge stress is calculated using the PVDF calibration curve shown in Figure 6. The gauge is effectively observing the derivative of the stress wave with a frequency response as defined by the gauge thickness and the sound speed of the PVDF ( $c_0 \approx 2700$  m/s) and is limited to  $\sim 10$  ns risetime.

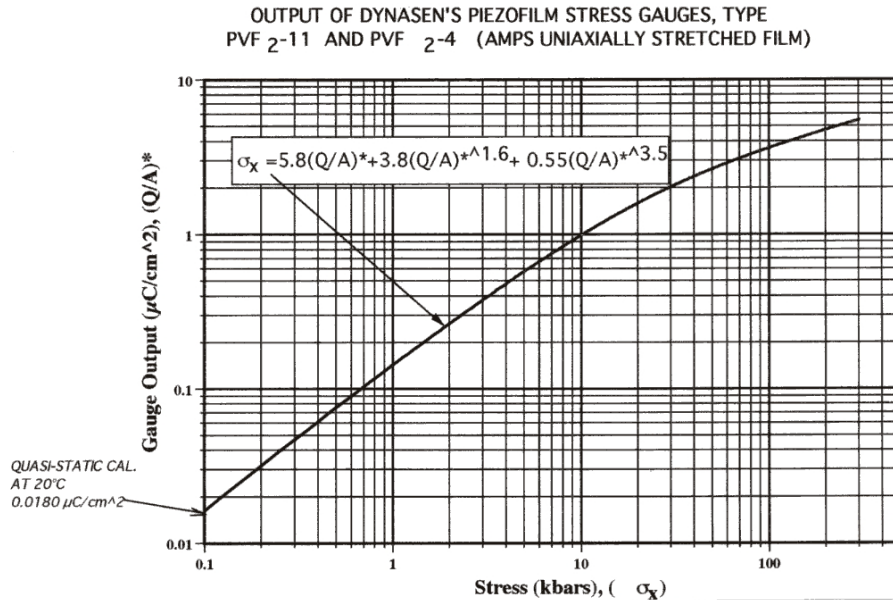


**Figure 6:** PVDF stress gauge calibration curve. Note that each gauge has a unique quasi-static calibration number (0.0180  $\mu\text{C}/\text{cm}^2$  is for reference).

## 3.2 Janus I

### 3.2.1 Test Plan

The objectives for the first test series on Janus (week of 14 Nov, 2011) were to a) establish operation of the PDI and PVDF diagnostics, b) measure the laser beam profile at the target, c) establish standard operations for first proof experiments and finally d) obtain data to compare with previous experiments (Kevin, et al, 2006).

### 3.2.2 Targets

All the targets used for Janus I were Al 6061 disks with thickness of nominally 954 microns or 783 microns. The thicknesses were measured using Jim Emig's digital micrometer. The aluminum disks were standard off the shelf aluminum sheets machined to the required diameter for the holder assembly (~25 mm). There was minimum surface preparation of the front (laser interaction) surface and no preparation of the back surface of the target other than cleaning with alcohol solvent. The minimum surface preparation consisted of polishing the aluminum with a microfinish sanding sheet, 2500 grit from McMaster-Carr(item 4611A311) in a figure eight motion for approximately 3-5 minutes using alcohol lubricant. The last four data shots used the aluminum disks with the ~3mm PMMA epoxied to the back. For all the data shots with the PDI system, the laser was looking at the back surface of the aluminum. One data shot was with the PVDF gauge with the target configuration as described in 3.1.4.

### 3.2.3 Experimental Results

For Janus I, the first three days (10, 11 & 14 Nov, 2011) were for training, setup and learning the laser operation. The first data shot was on Monday, 14Nov at 6:30PM (D1111141830). The emphasis for the first few days was characterization of the Janus beam spot intensity pattern using the Spiricon camera on loan from AFRL from Capt. Chris Vergien and using a calorimeter supplied by the JLF to cross calibrate the laser energy to our system to a reading on the E\_monitor in the laser bay (15.62 J/mJ).

The results of the Spiricon camera are shown in Figure 7 for four different laser spot diameters. The figures show vertical and horizontal intensity lineouts. It is interesting to note that for the larger diameter case (~6.43mm) that the beam intensity is relatively flat with increasing relative intensity changes as the spot gets smaller, but becoming very smooth at ~1mm and also showing rather high relative intensity in an outer ring.

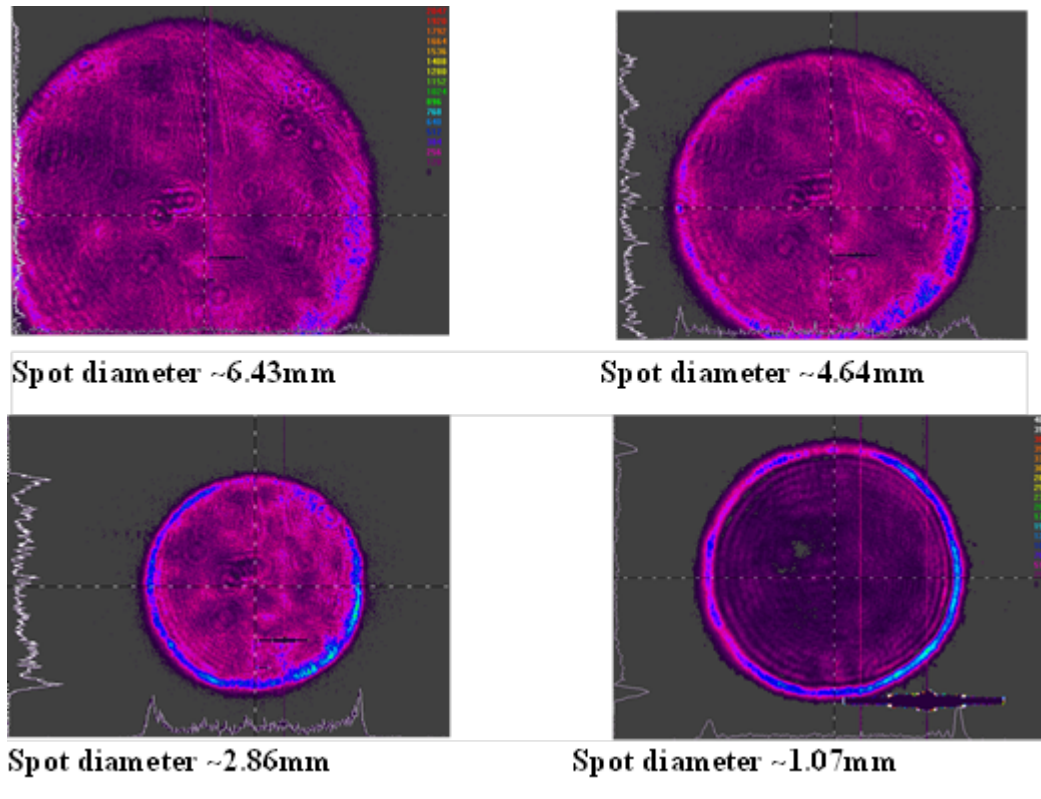


Figure 7: Images from the Spiricon camera of the laser spot size and relative intensity profile

Table 1 shows the final shot matrix for Janus I. A calorimeter was added after the 1<sup>st</sup> shot for calibration of the laser bay energy monitor. Post shot estimate of Shot 1 (D1111141830) is 50J. Shot 7 (D1111161521) was likely just a rod shot. A photodiode was mounted off-axis to the laser beam to monitor to laser pulse width. For all shots with the photodiode the laser pulsewidth was approximately 1.34ns FWHM and it was assumed to be the case for all the shots.

**Table 1: Janus I Shot Matrix**

Shot #	S/N	Target type	Shot energy (J)	Energy to Target (J)	pulse width (ns)	Average dia (mm)	Fluence (J/cm <sup>2</sup> )	Intensity (W/cm <sup>2</sup> )	inner dia. meas. (mm)	E_monitor reading (mJ)	Photo-diode signal (V)
1	D1111141830	954 um Al	50	45	1.34	11.729	41.7	3.11E+10	11.260	unknown	--
2	D1111151229	calorimeter	19.3	19.3	1.34		--	--	n/a	unknown	--
3	D1111151442	calorimeter	4.5	4.5	1.34		--	--	n/a	unknown	--
4	D1111151500	calorimeter	3.7	3.7	1.34		--	--	n/a	unknown	--
5	D1111151750	calorimeter	132.58	132.58	1.34		--	--	n/a	unknown	--
6	D1111161126	958 um Al	128.40	115.56	1.34	6.988	301.3	2.25E+11	6.625	8.22	0.300
7	D1111161521	958 um Al	5.50	4.95	1.34	7.305	11.8	8.81E+09	7.305	n/a	0.013
8	D1111161717	954 um Al	125.58	113.03	1.34	7.223	275.9	2.06E+11	7.155	8.04	0.348
9	D1111161837	954 um Al + 3 mm PMMA	154.95	139.46	1.34	7.103	352.0	2.63E+11	6.680	9.92	0.376
10	D1111171000	calorimeter	131.52	118.37	1.34		--	--	n/a	8.42	offline
11	D1111171320	954 um Al + 3 mm PMMA PVDF	130.90	117.81	1.34	11.098	121.8	9.09E+10	10.635	8.38	0.330
12	D1111171506	954 um Al + 3 mm PMMA	126.83	114.15	1.34	10.75	125.8	9.39E+10	10.75	8.12	0.302
13	D1111171717	783 um Al + 3 mm PMMA	126.99	114.29	1.34	6.185	380.4	2.84E+11	6.455	8.13	0.323

The PDI system recorded data on every shot where it was used. The results are shown in Table 2. In principal, interpretation of the displacement record should yield a good measure of the total impulse. The PDI measures the rear surface displacement versus time and then the derivative yields the rear surface velocity versus time. However, Figures 8 & 9 shows the PDI data from nominally the same test conditions, but shot\_1126 indicates a total impulse of ~300 taps, where shot\_1717 shows a total impulse of ~156 taps. The first step and the slope of the displacement versus time are clearly different, whereas the peaks of the velocity records are very similar. The difference is seen in the measured velocity dispersion after the peak. The reasons for the observed differences could be in lack of reproducibility in the target, changes in the laser intensity and/or intensity profile, or with uncertainties in the PDI system. Clearly this points out need to control variables, and test conditions for future experiments.

**Table 2: Test Results**

Shot	Fluence	I	1st step	Taps	(I...)meas	Cm(meas)
D111114_1830	41.7	3.11E+10	0.54	44	120.0	1.07
D111116_1126	301.3	2.25E+11	3.50	302	868.5	1.00
D111116_1717	275.9	2.06E+11	1.80	156	795.1	0.57
D111116_1837	352.0	2.63E+11	1.62	140	1014.4	0.40
D111117_1505	125.8	9.39E+10	1.64	168	362.5	1.34
D111117_1717	380.4	2.84E+11	3.55	362	1096.3	0.95

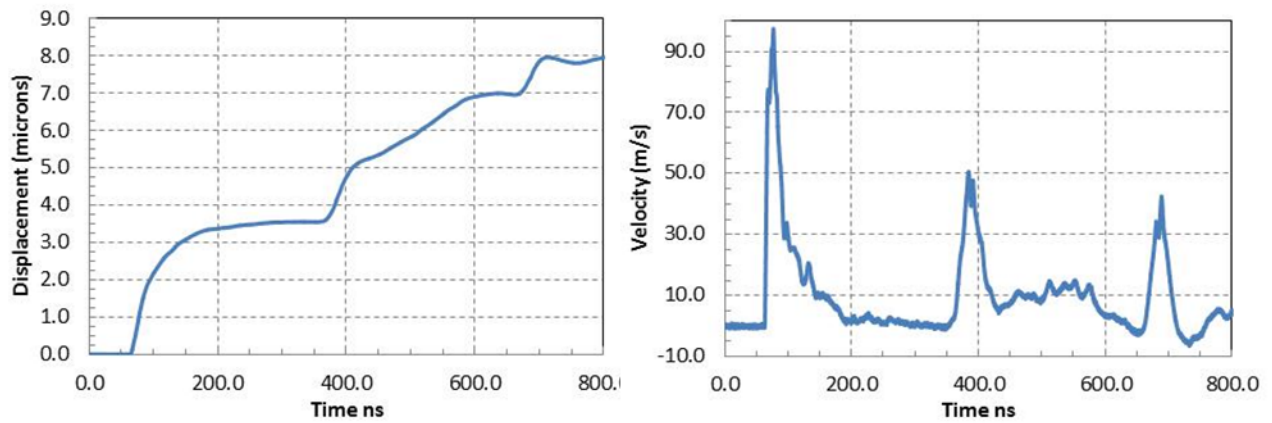


Figure 8: PDI measurement on shot D111116\_1126

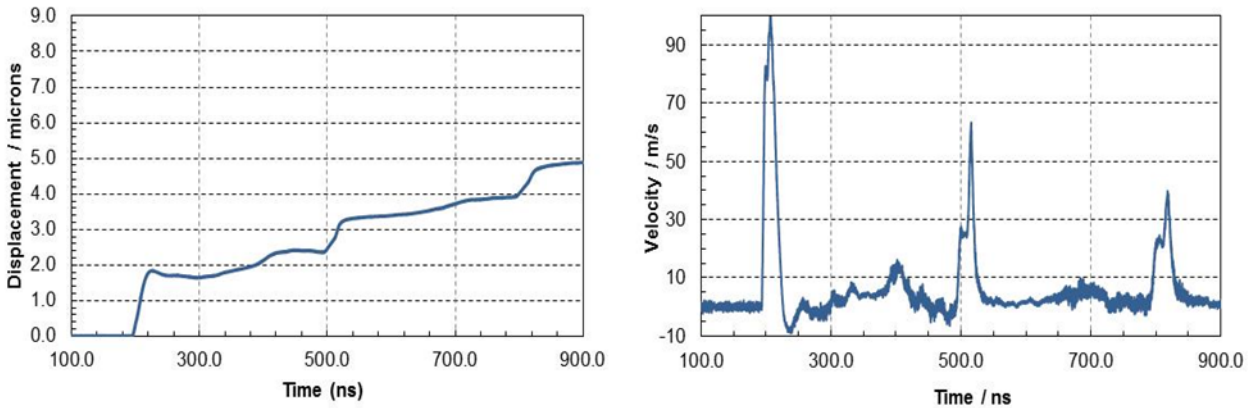


Figure 9: PDI measurement on shot D111117\_1717

The measured coupling coefficients are plotted in the graph shown in Figure 10. The measured results compared favorably to the empirical graph from Phipps and with the previous data by Fournier.

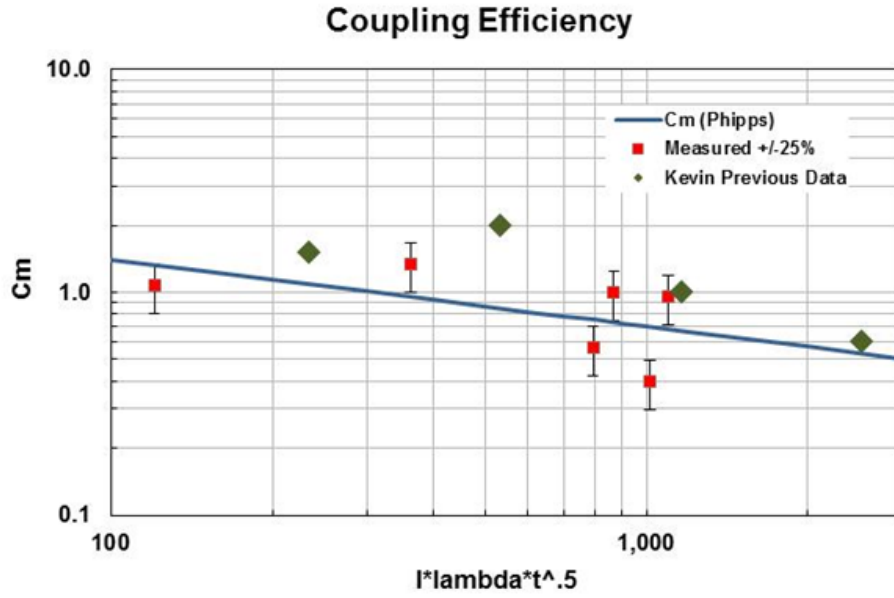
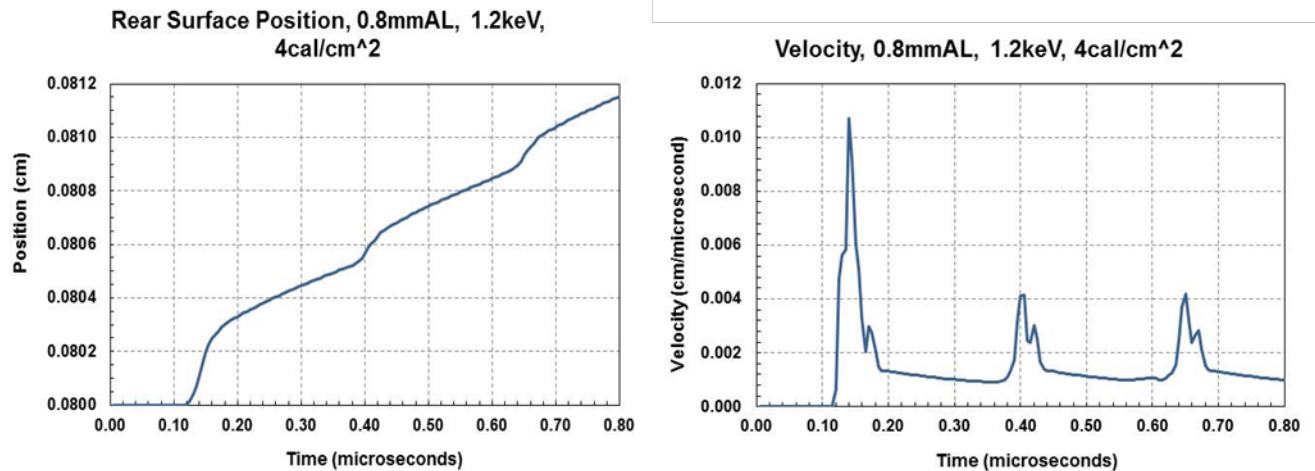


Figure 10: Laser impulse coupling efficiencies from Janus I data.



Figure 11: Post-shot photo of laser imprint onto front of aluminum target for shot 16-1126.



**Figure 12:** WONDY hydrocode results assuming 1.2 keV x-ray irradiation, 4 cal/cm<sup>2</sup>, 1.5 ns FWHM

### 3.2.4 M&S

Pre- and post-test modeling using a 1-D hydrocode was performed using the TSRTk from DTRA which has a nice GUI and uses either the WONDY or PUFF-TFT codes. The input parameters, EOS and zoning will be described in later reports. One of the limitations of the toolkit is that radiation input is limited to x-rays with energies greater than 1 keV. Figure 11 shows results assuming Al-6061, 800 microns thick, with radiation input of a single 1.2 keV x-ray, 1.5 ns pulse width and 4 cal/cm<sup>2</sup> (~16.86 J/cm<sup>2</sup>). The total calculated impulse is 300 taps. This calculation compares favorably with the experimental results shown in Figure 8. Figure 13 shows a later calculation with 950 micron Al, 5 cal/cm<sup>2</sup>, overlaid with shot 16-1126 showing excellent agreement with the velocity height and also the pulse shape.

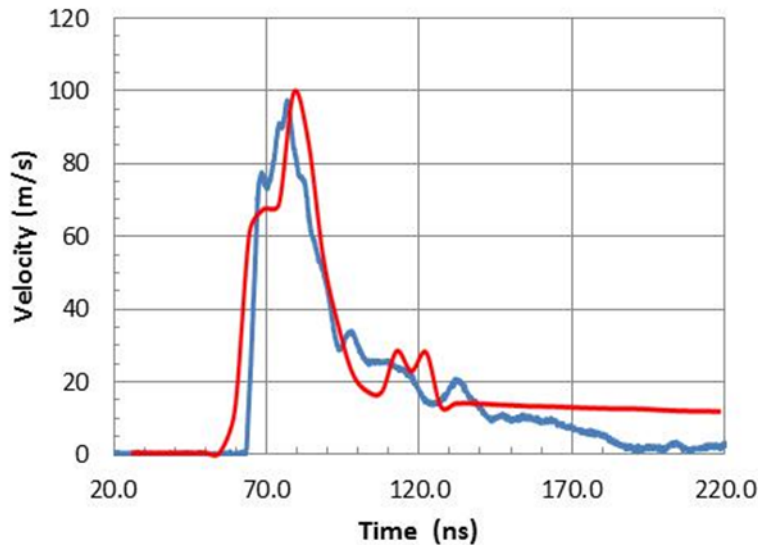


**Figure 13:** Overlay of WONDY code results in red with the observed velocity profile from shot 16-1126.

### 3.2.5 Discussion

The first test series, Janus I, accomplished all the pre-experimental goals. These included a) established operation of the PDI and PVDF diagnostics, b) measured the laser beam profile at the target, c) established standard operations for first proof experiments and finally d) obtained data to compare with previous experiments (Kevin, et al, 2006). The PDI system provided good, highly-time-resolved data. The one shot with the PVDF gauge provided good peak signals, but we are concerned that the need to integrate signals makes them prone to noise and small baseline shifts. For the next test series, higher time resolution ( $>1$  GS/s) would be desired.

For the next test series it is suggested that debris shields may be needed to prevent laser window damage. The repeated shots on aluminum targets may be depositing a thin layer of Al on the window that eventually causes it to break down. Un-explained differences in the data from nominally the same test conditions needs to be addressed for the next test series. This could be from a lack of reproducibility in the target, changes the laser intensity and/or intensity profile or with uncertainties the PDI system. Target surface finish needs to be better controlled and characterized preshot. Clearly this points out need to control variables, and test conditions for future experiments. The next step will include developing and testing a surface treatment to increase the impulse coupling coefficient.

### 3.3 Janus II

The second test series (Janus II) was conducted during the week of 14 May 2012. AWE was not able to support experiments, thus this test series was conducted without the use of the PDI diagnostics and all tests used targets with the PVDF gauge configuration as shown in Figures 3&4.

#### 3.3.1 Test Plan

The objectives of the second test series followed logically from the first series. First, re-establish last test conditions and measurement conditions (make improvements as needed). Next measure impulse with aluminum target, and compare to Al target with a simple 'laser coupling' layer, then compare to Al target with both the laser coupling layer and several thicknesses of clear plastic 'tamping' layers.

The determination of the laser beam spot size versus optical rail position was re-measured and the lens to target position was established to achieve ~7.6mm diameter laser spot for all the tests. Note for Janus II, there was a new final focus optic and an extension to the target chamber as shown in Figure 1. For these experiments, the lens focal length was assumed to be 1000mm and the beam diameter was assumed to be 62.5mm (f/16).

#### 3.3.2 Targets

As indicated above, all targets for Janus II used the PVDF configuration as shown in Figures 3&4. The PVDF gauge thickness (see Figure 5) was ~29.54 microns with a 25 micron layer of Kapton polyimide above and below the PVDF layers. The gauge was epoxied to the back plate of the Al target. The estimated epoxy thickness was order of 10-15 microns per layer.

The 'laser coupling' layer was Black Kapton(R) (made by DuPont and listed Kapton XC, black anti-static polyimide film). This is a polyimide film, electrically conductive, 0.001" thick (from McMaster-Carr, item 2271K69). The 'tamping' layers were clear plastic overlays, 0.0005", 0.001" and 0.004" moisture-resistant polyester film purchased from McMaster-Carr (items 8567K102, 8567K12 & 8567K42, respectively).

**Table 3: Janus II Shot Matrix**

#	S/N	Target type	Shot Request (J)	Shot energy (J)	Energy to Target (J)	pulse width (ns)	Average dia (mm)	Fluence (J/cm <sup>2</sup> )	Intensity (W/cm <sup>2</sup> )	Measured peak stress	Impulse at t <sub>0</sub> +0.9us taps
1	D051512-0905	783 micron Al disk	125	25.0	23.5	6	5.665	93.2	1.55E+10	0.0	
2	D051512-1143	783 micron Al disk w PVDF w PMMA G4P1 0.0146 uC/cm <sup>2</sup>	125	138.5	130.2	6	7.585	288.2	4.8E+10	1.2	196
3	D051512-1517	783 micron Al disk w PVDF w PMMA G2P1 0.0155 uC/cm <sup>2</sup>	125	160.6	151.0	6	7.69	325.0	5.42E+10	1.2	
4	D051512-1827	956 micron Al disk w PVDF w PMMA G3P2 0.0189 uC/cm <sup>2</sup>	125	138.0	129.7	6	8.4	234.1	3.9E+10	1.6	196
5	D051612-0859	504 um Al disk + 27um black Kapton + ~12um epoxy	125	93.2	87.6	6	8.85	142.4	2.37E+10	0.0	
6	D051612-1053	956 um Al disk w 27um black Kapton + PVDF + PMMA G2P2 0.0187 uC/cm <sup>2</sup>	125	98.4	92.5	6	8.4	166.9	2.78E+10	1.7	225
7	D051612-1326	956 um Al disk w 15um poly w 27um black Kapton + PVDF + PMMA G6P1 0.0157 uC/cm <sup>2</sup> <i>changed atten from 2X to 5X</i>	125	107.0	100.6	6	9.23	150.3	2.51E+10	9.3	754
8	D051612-1442	956 um Al disk w 26um poly w 27um black Kapton + PVDF + PMMA G1P2 0.0189 uC/cm <sup>2</sup> <i>added 2x, atten is now 10X</i>	125	96.0	90.2	6	8.46	160.5	2.68E+10	7.7	580
9	D051612-1533	956 um Al disk w 100um poly w 27um black Kapton + PVDF + PMMA G3P2 0.0189 uC/cm <sup>2</sup> <i>atten is now 5X</i>	125	114.0	107.2	6	7.125	268.8	4.48E+10	4.5	755
10	D051712-0905	956 um Al disk w 26um poly w 27um black Kapton + PVDF + PMMA G1P1 0.0163 uC/cm <sup>2</sup> <i>atten is now 5X</i>	125	147.0	138.2	6	8.01	274.2	4.57E+10	6.0	715
11	D051712-1044	956 um Al disk w 15um poly w 27um black Kapton + PVDF + PMMA G3P1 0.0142 uC/cm <sup>2</sup> <i>atten is now 5X</i>	125	135.0	126.9	6	8.46	225.8	3.76E+10	7.0	754
12	D051712-1355	783 um Al disk w 15um poly w 27um black Kapton + PVDF + PMMA G2P2 0.0159 uC/cm <sup>2</sup> <i>atten is now 5X</i>	125	154.0	144.8	6	8.46	257.5	4.29E+10	7.8	684

### 3.3.3 Experimental Results

The Janus II shot matrix is shown in Table 3. There were a total of 12 shots, ten using the PVDF gauge. Figure 14 is a post-shot photo of one of the targets with the black Kapton and with a thin polyester layer. The polyester layer is completely removed and some, but not all of the black Kapton layer is gone. The ablation did not reach the Al surface in any of the shots with the black Kapton in place. Post-shot look after the third shot with the coupling/tamping layers (12-1533) showed that the debris shield approximately 50 cm from the target, inside the target chamber was shattered. Figure 15 shows a photo of the shattered shield. The shield was replaced, but we broke the 2<sup>nd</sup> shield on the next shot (17-0905). For the rest of the shots, the target was angled ~21° from the laser axis and no further debris was observed on the window.



**Figure 14:** Post-shot photo of target showing the polyester tamping layer completely removed and with some of the black Kapton coupling laser remaining.



**Figure 15:** Photo of shattered glass debris shield after shot 16-1533.

Figure 16 shows a compilation of the stress gauge results for this test series. Note that there were no statistical variation between the bare Al target and the targets with the added Black Kapton. All the targets with the added ‘tamping’ layer showed significant increases in the peak stress and the stress profile. Figure 17 shows the integrals of the measured stress profiles to estimate the total impulse. The use of the coupling/tamping layers increased the impulse by more than 3.5X. Of interest, is the change in the stress profile with the thickest tamping layer (100 micron polyester). The peak stress is lower than that with thinner layers but the stress width is much broader, leading to the conclusion that the added coupling/tamping layers can be designed to both increase the coupling efficiency and control the stress pulse shape.

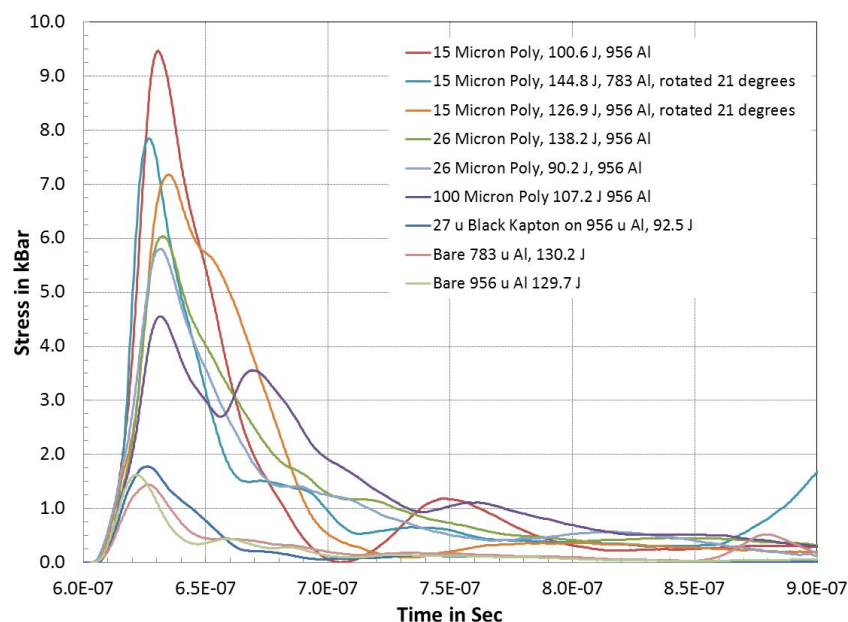


**Figure 16:** Compilation of stress gauge results showing ~6X increased peak stress measured at the gauge with added coupling/tamping layers.

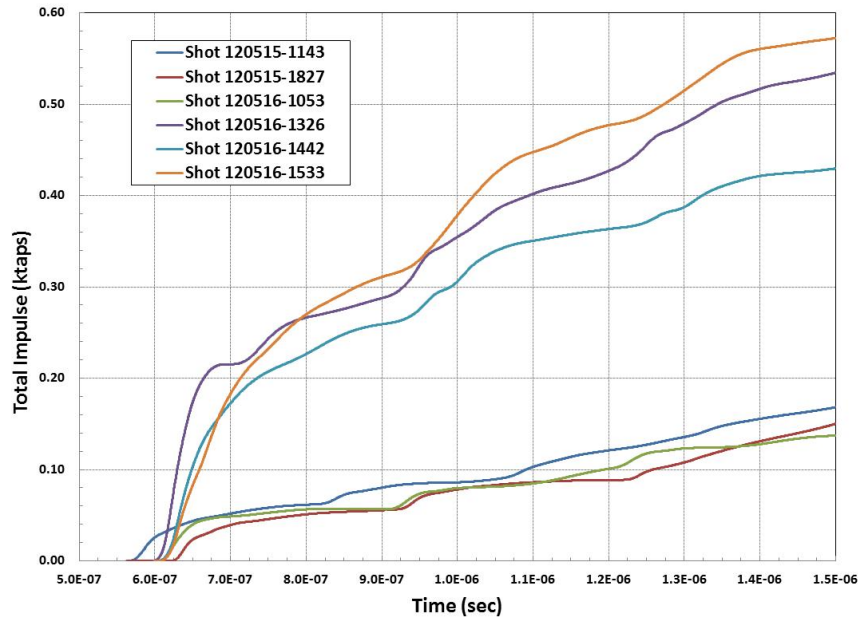


**Figure 17:** Integrals of the measured stress profiles to estimate the total impulse. The use of the coupling/tamping layers increased the impulse by factor  $>3.5X$ .

### 3.3.4 M&S

As with the previous test series, pre- and post-test modeling using a 1-D hydrocode was performed using the TSRTk from DTRA. The input parameters, EOS and zoning will be described in later reports. Figure 18 shows results assuming Al-6061, 954 microns thick back by 3 mm of PMMA. The calculated stresses are at approximately 50 microns into the PMMA from the Al-PMMA interface. For these modeling runs, the zoning in the PMMA was  $\sim 15$  microns to replicate the response of the PVDF gauge which has a sensitive thickness of  $\sim 28$  microns. The shock width in the PMMA without the coupling & tamping layers is of order 80 microns, and with the coupling/tamping layer is of order 150 – 250 microns.

Note that the two runs with incident x-ray energies of  $15 \text{ cal/cm}^2$  both show significant broadening of the observed stress wave. This is due to delayed material blowoff at the front surface. The peak stress from the blackbody source is lower versus that calculated with 1.7 keV monoenergetic x-ray input as the blackbody source produces more in-depth heating allowing for some stress relief at the front surface. The calculated total impulse for the  $15 \text{ cal/cm}^2$  cases is approximately 825 taps. Additional calculations indicate that with  $30 \text{ cal/cm}^2$  incident the calculated total impulse is  $\sim 1250$  taps.

Figure 19 shows an overlay of these modeling results with the observed stress profiles. The modeling shows remarkably good agreement with the experimental data, implying that the peak stresses has increased with the coupling/tamping layers  $\sim 5.8X$ . Using the measured total impulse data, Figure 20 shows the calculated improvement in the coupling coefficients with the coupling/tamping layers of order 3-4X.

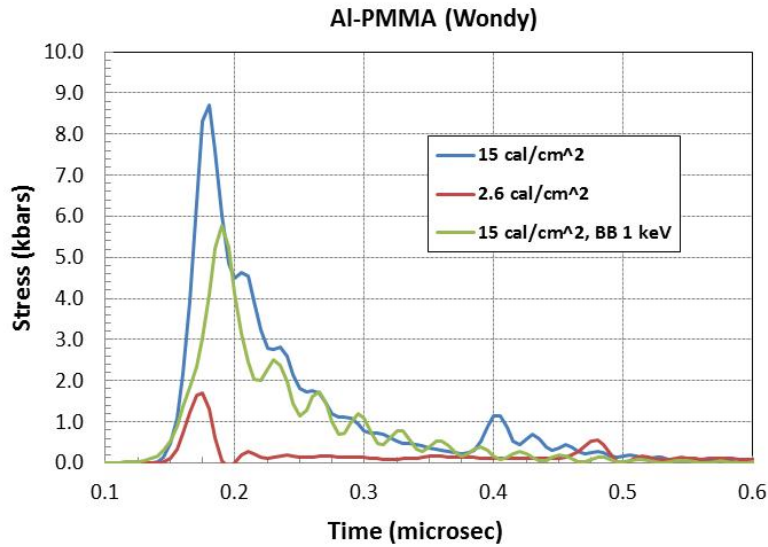


**Figure 18:** Modeling results with mono-energetic x-ray (1.7 keV) versus a 1 keV blackbody source.

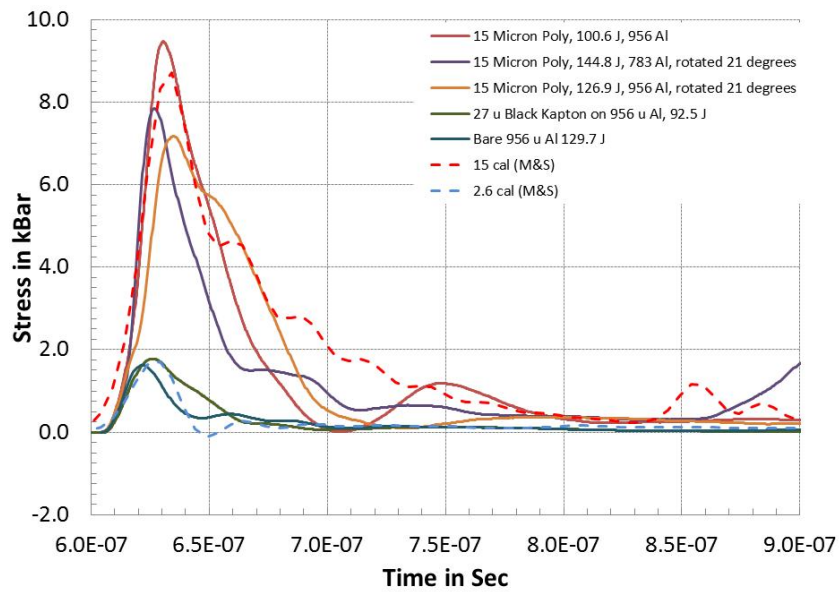


**Figure 19:** Overlay of model results versus observed stress profiles at the stress gauge position with/without added coupling/tamping layers

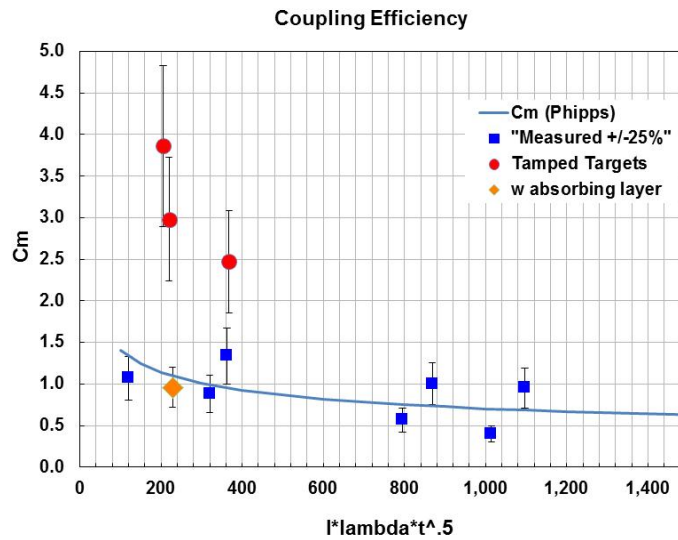


**Figure 10:** Measured laser coupling coefficients with/without coupling/tamping layers on Al

## 4 Conclusions

These initial experimental results are consistent with previous experiments and the PDI and targets with PVDF gauges successfully obtained data. The addition of simple absorbing-tamping layer(s) has shown  $\sim 4X$  improvement in total impulse and  $\sim 6X$  increase in the peak stress. The different thicknesses of tamping layers have also shown variations in initial stress width with demonstrated increases from  $\sim 30$ - $50$  ns to over  $200$  ns versus no tamping layer. Of note, these simple added layers should be applicable to any material, thus allowing controlled impulse testing on material and configuration of interest.

We must keep in mind that these results, though they look very promising, need to be optimized. The next step is a combined modeling & simulation with experimental campaigns. We can use these results to extrapolate to tests with bigger laser systems. Assuming of order 94% of the laser energy to the area of interest and that we can optimize coupling layers to achieve  $\sim 5X$  improvement in laser coupling efficiency, then with UK ORION at 5 beams overlapped ( $\sim 2kJ$  &  $1.88kJ$  to target), should induce order of  $1.2$  kilotaps impulse with test object diameter of  $\sim 32mm$ . With one quad of NIF we should be able to produce similar impulses to test objects with diameters of order  $90$  mm. These potential test capabilities are shown in Table 4.

**Table 1:** Estimated test object dimensions assuming  $5X$  improvement in laser coupling coefficients

Laser	Shot energy (J)	pulse width (ns)	Test diameter (mm)	Test Area (cm <sup>2</sup> )	Fluence (J/cm <sup>2</sup> )	Intensity (W/cm <sup>2</sup> )	Impulse (taps)
Orion	2200	5.0	32.0	8.0	257.1	5.14E+10	1204
NIF	15000	10.0	90.0	63.6	221.6	2.22E+10	1204
NIF	45000	10.0	155.0	188.6	224.2	2.24E+10	1213

## Information on Interferometry system hardware, setup etc for use on Janus

### **Laser Specs:**

Supplier: IPG Photonics  
 Model: ELR-2-1550-SF  
 Mode: CW  
 Max Output: 2.4W  
 Emission: 1550.6nm  
 Linewidth: <30kHz  
 Out of band: -32dB

Fiber type: SMF-28  
 Fiber termination: FC/APC

Supply Voltage: 100-240 VAC  
 Power consumption: <120 W

Dimensions: 19" rack mountable (483X133X424 mm)

Safety: Laser output requires the use of a key which would remain in my possession. Also has an interlock connection on the back to link in with any required interlocking the facility has.

\*\*\*Note: Laser may not be this exact model but will be very similar.

### **Method of Operation:**

Laser would be run operated at a low power output of ~150-250 mW (dependent on reflection quality from target). The fiber output from the laser is connected to the 'interferometry box'.

This box has a single fiber output which would lead to the target location where, via some form of vacuum feedthrough, would connect to a probe which is aligned to our target materials. The laser power from this box could be limited via an attenuator within the box to class I levels (which is 30mW for IR free space lasers) if necessary, though even without attenuation it would be less than half the power entering the box.

The box would have 3 SMA connectors which would need to be connected to a suitable oscilloscope and also requires a +/- 15V input which is supplied via a separate DC power supply.

### **So the laser route is:**

Laser to box: 150-250mW fully enclosed in fiber  
 Box to feed through: Can be 30mW (Class I) if needed but fully enclosed in fiber  
 Feedthrough to probe: Can be 30mW (Class I) if needed but fully enclosed in fiber

## References

*LASNEX calculations of laser-coupling coefficients for Al targets*, K. B. Fournier, presentation to Missile Defense Agency (UCRL-PRES-226849), 7 Dec 2006.

*Data Report on Material Ablation and Shock Pressure Measurements at ZBL*, E. Smith, B. Bonahoom, C. De La Cruz (UCRL-TR-227274), Jan 2007.

*Impulse coupling to targets in vacuum by KrF, HF, and CO<sub>2</sub> single-pulse lasers*, C. R. Phipps, et. al., J. Appl. Phys. **64** (3), 1 August 1988.

*Time-Resolved Impulse Measurements on SATURN*, S. C. Jones, et. al., presented to the Hardened Electronics and Radiation Technologies (HEART) Conference, March 2009. *Photonic Displacement Interferometer Thermomechanical Shock (TMS) And Early Thermostructural Response (TSR) Measurement Applications*, Scott C. Jones, presented to the HEART Conference, March 2006.

*Measurement and Analysis of Pulsed Laser Generated Stress Waves in Epoxy and PMMA*, D. Newlander and S.F. Stone, Shock Compression of Condensed Matter, 1989.